Journal of Materials Chemistry B

Accepted Manuscript

ROYAL SOCIETY OF CHEMISTRY

www.rsc.org/materialsB

Cite this: DOI: 10.1039/c0xx00000x

www.rsc.org/xxxxxx

ARTICLE TYPE

Doxorubicin and Fe_3O_4 loaded albumin nanoparticles with folic acid modified dextran surface for tumor diagnosis and therapy

Hequn Hao[a,c], Qingming Ma[b], Fen He[b], Ping Yao[a]*

Received (in XXX, XXX) Xth XXXXXXXXX 20XX, Accepted Xth XXXXXXXXX 20XX

DOI: 10.1039/b000000x

In this study, multifunctional bovine serum albumin (BSA) nanoparticles were fabricated via a green approach with high efficiency. Folic acid (FA) was conjugated to dextran (DEX) through an esterification reaction, and BSA-DEX-FA conjugate was produced by Maillard reaction. Superparamagnetic Fe_3O_4 nanocrystals with a size about 10 nm were loaded into BSA-DEX-FA nanoparticles through a heat treatment to induce BSA gelation. Doxorubicin (DOX) was loaded into Fe_3O_4/BSA-DEX-FA nanoparticles by a diffusion process. Fe_3O_4/BSA-DEX-FA and DOX/Fe_3O_4/BSA-DEX-FA nanoparticles have a size about 100 nm, good stability, superior transversal R_2 relaxation rate of larger than 360 $(mM)^{-1}s^{-1}$, as well as FA receptor-targeted and magnetically guided functions. Fe_3O_4/BSA-DEX-FA nanoparticles have excellent biocompatibility. By application of an external magnetic field close to tumor, DOX/Fe_3O_4/BSA-DEX-FA nanoparticles can effectively enhance the tumor inhibition rate and prolong the life time of H22 tumor-bearing mice, and Fe_3O_4/BSA-DEX-FA nanoparticles can significantly improve the tumor MRI of KB tumor-bearing mice. This study demonstrates that Fe_3O_4/BSA-DEX-FA and DOX/Fe_3O_4/BSA-DEX-FA nanoparticles are suitable systems for tumor diagnosis and therapy.

1 Introduction

Cancer is among the top killer diseases in the world. For the majority of patients with advanced stage of cancer, the treatment is limited to chemotherapy or radiation.[1,2] Because chemotherapy lacks selectivity for cancer and has severe toxicity to normal tissues, tumor-targeted delivery of antitumor drugs is an promising strategy for chemotherapy. Recently, multifunctional nanoparticles, which combine multiple therapeutic functions and imaging capabilities together, have received great research attention.[3-6] Superparamagnetic iron oxide nanoparticles (SPIONs) have low toxicity, good biocompatibility and biodegradability, as well as high sensitivity.[7,8] Nanoparticles containing SPIONs have wide potential applications, such as remotely controlled drug delivery and hyperthermia by manipulating external magnetic field for tumor therapy, and magnetic resonance imaging (MRI) for tumor diagnosis.[9-12] For example, Huang et al developed folate (FA) receptor-mediated and magnetically guided doxorubicin (DOX)-loaded SPIONs@F127-PLA-FA nanomicelles.[13] In VX2 tumor-bearing male New Zealand white rabbit treatment, the nanomicelles were guided into tumor site more efficiently by application of an external magnetic field. Wang et al developed a multifunctional nanocomposite by coating SPIONs with polymer polypyrrole (PPy) and then with PEG.[6] In their system, Fe_3O_4 core is useful for magnetically controlled drug delivery as well as MRI contrast; PPy shell is able to load DOX and also exhibits strong photothermal effect. The system showed outstanding synergistic antitumor effect *in vivo*. Gianella et al developed a multimodal "theranostic" platform based on oil-in-water nanoemulsions, which carried iron oxide nanocrystals for MRI, fluorescent dye Cy7 for NIRF imaging, and hydrophobic glucocorticoid prednisolone acetate valerate for therapeutic purposes.[14] *In vivo* administration and MRI and NIRF imaging for tumor-bearing nude mice showed significant nanoparticle accumulation in tumor and potent tumor inhibitory effect.

Albumin has been widely used for drug delivery owing to its biodegradable, biocompatible, and nontoxic properties[15-17] after the success of Abraxane®, paclitaxel loaded human serum albumin (HSA) nanoparticles.[18] For example, Wagner et al synthesized DOX loaded HSA nanoparticles with monoclonal antibody DI17E6 for specifically targeting αvβ3 integrin positive melanoma cells.[19] Bae et al produced DOX loaded HSA nanoparticles modified with TNF-related apoptosis-inducing ligand and transferrin for targeting multiple tumor types.[20] Wang et al prepared boronic acid-rich nanoparticles composed of bovine serum albumin (BSA) and poly(N-3-acrylamidophenylboronic acid) for liver-targeted delivery of DOX.[21] Zhang et al produced BSA/SPION hybrid nanoclusters for liver-specific MRI.[22] Previously, we produced DOX loaded BSA nanoparticles with FA modified dextran (DEX) surface for targeting FA receptor-overexpressed tumor.[23]

In this study, we combine the merits of SPIONs and albumin nanoparticles together to fabricate multifunctional nanoparticles for tumor diagnosis and therapy. We used BSA nanoparticles as matrices to load superparamagnetic Fe_3O_4 nanocrystals and DOX. DOX is an anthracycline anticancer drug with broad-spectrum antitumor activity.[24] Fe_3O_4 nanocrystals are used for magnetically

guided DOX delivery and MRI contrast agent. Furthermore, the Fe_3O_4 and DOX loaded BSA nanoparticles have FA modified DEX surface. The DEX surface endows the nanoparticles with excellent dispersibility in aqueous solution as well as the "stealth" property which prolongs the circulation time of the nanoparticles in blood stream.[25] The FA groups conjugated to DEX enable the nanoparticles to target FA receptor-overexpressed tumor. In this study, we developed a green approach to fabricate Fe_3O_4/BSA-DEX-FA and DOX/Fe_3O_4/BSA-DEX-FA nanoparticles. The nanoparticles were characterized by various techniques including *in vitro* and *in vivo* antitumor activity and MRI evaluations.

2 Materials and methods

2.1 Materials

Doxorubicin hydrochloride (DOX·HCl, 99.0%) was from Zhejiang Hisun Pharmaceutical Co. Ltd. BSA (fraction V, 99%) and dextran (DEX, molecular weight 10 kDa) were supplied by Amresco Inc. Folic acid (FA, 98%) was purchased from Sigma. Dimethyl sulfoxide (DMSO, 99%, Sinopharm Chemical Reagent Co.) was dried over CaH_2 and then distilled under vacuum before use. N, N′-dicyclohexylcarbodiimide (DCC, 98%), 4-(dimethylamino) pyridine (DMAP, 98%), Iron(III) chloride hexahydrate ($FeCl_3·6H_2O$, analytical grade), and iron(II) sulfate heptahydrate ($FeSO_4·7H_2O$, analytical grade) were purchased from Sinopharm Chemical Reagent Co. Human oral squamous carcinoma KB cell line was from American Type Culture Collection. Dulbecco's modified Eagle's medium (DMEM) cell culture and fetal bovine serum were from GIBCO BRL Life Technologies Inc. MTS [3-(4,5-dimethylthiazol-2-yl)-5-(3-carboxy-methoxyphenyl)-2-(4-sulfophenyl)-2H-tetrazolium] was from Promega Company. All other chemicals were analytical grade and used directly. All aqueous solutions were prepared using deionized water having a resistance of 18 MΩ.

2.2 Preparation of DOX and Fe_3O_4 loaded BSA-DEX-FA (DOX/Fe_3O_4/BSA-DEX-FA) nanoparticles

Superparamagnetic Fe_3O_4 nanocrystals were synthesized using a coprecipitation technique of divalent and trivalent iron salts in alkaline medium[26] with some modifications. Under stir and nitrogen atmosphere, 0.04 mol $FeCl_3·6H_2O$ and 0.02 mol $FeSO_4·7H_2O$ were dissolved together in 100 mL water for 30 min, a 50 mL of 10 M NaOH solution was added dropwise within 30 min, the mixed solution was kept at room temperature for 1 h and then kept at 90 °C for 2 h in succession. The produced Fe_3O_4 nanocrystals were collected by an external magnetic field and then resuspended in water repeatedly until the pH of the supernatant changed to neutral. The purified Fe_3O_4 nanocrystals were obtained after lyophilization.

DEX-FA and BSA-DEX-FA conjugates were synthesized as described previously.[23,27] FA was conjugated to DEX via an esterification. Subsequently, DEX-FA and free DEX were synchronously conjugated to BSA by Maillard reaction with a molar ratio of BSA to total DEX 1:4 and a molar ratio of DEX-FA to DEX 1:5. Similarly, BSA-DEX conjugate without FA was prepared from BSA and DEX with a molar ratio of BSA to DEX 1:4.

BSA-DEX-FA conjugate was dissolved in 6 mL water with BSA concentration of 5 mg/mL; 12 mg Fe_3O_4 nanocrystals were added into the conjugate solution. The mixed solution was adjusted to pH 4.0, stirred in the dark for 12 h, and then heated at 80 °C for 1 h to produce Fe_3O_4 loaded BSA-DEX-FA (Fe_3O_4/BSA-DEX-FA) nanoparticles.

DOX·HCl aqueous solution was added into Fe_3O_4/BSA-DEX-FA solution at room temperature with a weight ratio of DOX to BSA 1:4 and final DOX concentration of 1.25 mg/mL. The mixture was stirred in the dark for 12 h, adjusted to pH 7.4, and stirred in the dark for another 12 h in succession to load DOX in Fe_3O_4/BSA-DEX-FA nanoparticles. After centrifugation at 5000 rpm for 10 min to remove large particles, stable DOX/Fe_3O_4/BSA-DEX-FA nanoparticle dispersion was obtained and stored at 4 °C before use. DOX/Fe_3O_4/BSA-DEX nanoparticles without FA were produced from BSA-DEX instead of BSA-DEX-FA.

2.3 Characterizations of the nanoparticles

Dynamic light scattering (DLS) measurements were carried out at 25 °C on a laser light scattering spectrometer (ALV/CGS-8F, λ = 632.8 nm) at a fixed scattering angle of 90°. Apparent z-average hydrodynamic radius (R_h) and polydispersity index (PDI) were obtained by Cumulants analysis. DLS sample was prepared by diluting the nanoparticle solution to BSA concentration of 0.1 mg/mL. Transmission electron microscopy (TEM) observations of the nanoparticles were conducted on a Philips CM120 electron microscope. TEM sample was prepared by depositing diluted nanoparticle solution onto a carbon-coated copper grid and then drying the grid at room temperature. XRD patterns of the freeze-dried Fe_3O_4 nanocrystals were acquired on an x-ray powder diffractometer (X' pert PRO, PANalytical) at a rate of 0.05°/sec in a 2θ range of 20–80°. The iron content in the nanoparticles was analyzed on an inductively coupled plasma atomic emission spectrometer (ICP-AES, Hitachi P-4010). The ICP-AES sample was prepared by adding 0.1 mL nanoparticle solution into 2 mL concentrated hydrochloric acid (37%), heating the mixed solution at 60 °C for 2 h, and then diluting the solution to 8 mL with water. The magnetization curves of freeze-dried nanoparticles were measured on a magnetic property measurement system (MPMS SQUID VSM, Quantum Design) at 300 K under circulating magnetic field between -2×10^4 and 2×10^4 Oe.

The free DOX in DOX/Fe_3O_4/BSA-DEX-FA and DOX/Fe_3O_4/BSA-DEX nanoparticle solutions was separated using Amicon Ultra centrifugal filter (Ultracel 50 kDa, Millipore) and was collected in the ultrafiltrate. The adsorption of DOX on the ultrafiltration membrane was calibrated by a standard free DOX solution at the same condition. The absorption at 480 nm of the ultrafiltrate was measured on a spectrophotometer (Shimadzu UV-2550) to calculate the free DOX concentration. DOX working curve was obtained by standard DOX solutions with different DOX concentrations. DOX loading efficiency and loading amount were calculated using the following equations:

$$\text{Loading efficiency (\%)} = \frac{\text{DOX in feed} - \text{free DOX}}{\text{DOX in feed}} \times 100\%$$

$$\text{Loading amount (\%)} = \frac{\text{DOX in feed} - \text{free DOX}}{\text{conjugate in feed}} \times 100\%$$

2.4 *In vitro* DOX release from the nanoparticles

DOX release was investigated using a dialysis method. DOX/Fe_3O_4/BSA-DEX-FA or DOX/Fe_3O_4/BSA-DEX nanoparticle solution of 0.5 mL was dialyzed (cutoff molecular weight 14 kDa) against 24.5 mL release buffer at 37 °C in the dark. Periodically, 3 mL of the release buffer was taken out and the same volume of fresh buffer was added. The absorption at 480 nm of the release buffer was measured to calculate the DOX concentration.

2.5 *In vitro* cytotoxicity of the nanoparticles

Cell viability against DOX loaded nanoparticles was investigated by MTS assay. KB cells were seeded in 24-well plates and incubated in complete culture medium (DMEM medium supplemented with 10% fetal bovine serum and 100 IU/mL penicillin G sodium and 100 μg/mL streptomycin sulfate) at 37 °C and 5% CO_2 atmosphere. After 24 h incubation, the cells were treated with 0.5 mL/well fresh media containing free DOX, DOX/Fe_3O_4/BSA-DEX or DOX/Fe_3O_4/BSA-DEX-FA nanoparticles with different DOX concentrations in triplicate. The cells were incubated with an external magnetic field of 0.17 T under the plate or not for 12 h and then incubated without magnetic field for another 60 h. After incubation, the cell media were replaced by 120 μL fresh medium containing 16.7% MTS and the cells were incubated for another 2 h. Then, the optical density of the plates was read on a BioTek microplate reader. For time-dependent cell viability, the cells were treated with free DOX and DOX loaded nanoparticle solutions containing 1.0 μg/mL DOX for designed time.

2.6 *In vitro* MRI of the nanoparticles

T_2-weighted magnetic resonance (MR) images were acquired on a clinical MRI instrument (Siemens 3T Trio MRI system). The samples were prepared by suspending Fe_3O_4/BSA-DEX-FA or DOX/Fe_3O_4/BSA-DEX-FA nanoparticles in 1% agarose solutions with different iron concentrations. The parameters of T_2-weighted fast-recovery fast spin-echo (FR-FSE) sequence are as follows: TR, 3000 ms; TE, 13.2, 26.4, 52.8, 66.0, 79.2, 92.4, 105.6, 118.8, 132.0, 145.2 ms; matrix size, 640 × 640; slice thickness, 5 mm; field of view (FOV), 128 × 128 mm^2. Transversal (R_2) relaxation rates were calculated by linear fitting of $1/T_2$ (T_2, relaxation time) versus Fe concentration.

KB cells were seeded in 6-well plates and incubated in complete culture medium for 24 h. After being washed with phosphate buffered saline (PBS, pH 7.4), the cells were treated with 2 mL/well fresh media containing Fe_3O_4/BSA-DEX-FA nanoparticles with a iron concentration of 0.052 mg/mL and an external magnetic field of 0.17 T under the plate for 6 and 24 h. Subsequently, the cells were washed with PBS repeatedly, detached, transferred to centrifugal tubes, and resuspended in 1% agarose solutions to fix the cells for MRI. The imaging parameters are the same as described above.

2.7 *In vivo* antitumor efficacy of the nanoparticles

The animal experiments on tumor treatment of this study were performed at National Pharmaceutical Engineering Research Center in full compliance with the guidelines approved by Shanghai Administration of Experimental Animals. Free DOX solution of 1 mg/mL was prepared freshly before administration by dissolving DOX·HCl in sterile physiological saline injection. DOX/Fe_3O_4/BSA-DEX-FA nanoparticle solution was diluted to DOX concentration of 1 mg/mL with sterile physiological saline injection freshly before administration. Filtration sterilization was performed using 0.22 μm film for the free DOX and nanoparticle solutions.

ICR mice (18–22 g) from Sino-British SIPPR/BK Lab. Animal Ltd. were injected in right axilla with 3×10^6 H22 cells. The mice were randomly assigned to various treatment groups with five male and five female in each group. The treatment started after 3 days of the inoculation. Physiological saline injection, free DOX solution with DOX dose of 5 mg/kg every day, and DOX/Fe_3O_4/BSA-DEX-FA nanoparticle solution with DOX doses of 5, 8, and 10 mg/kg every day were separately injected via the tail veins for 5 days. After each administration, each mouse in DOX/Fe_3O_4/BSA-DEX-FA+field groups was immediately treated with an external magnetic field by binding a small magnet of 0.15 T closed to the tumor for 2 h. After 10 days of the inoculation, all mice were sacrificed by cervical dislocation; the solid tumors were taken out and weighed. The tumor inhibition rate (TIR) was calculated according to the following equation: TIR (%) = (1 − WT/WC) × 100%, where WT is the average tumor weight of the DOX treated group and WC is the average tumor weight of the physiological saline treated group.

For survivability study, the mice were injected in abdomen with 3×10^6 H22 cells. The mice were randomly assigned to various treatment groups with ten male in each group. The treatment started after 4 days of the inoculation. Physiological saline injection, free DOX solution with DOX dose of 5 mg/kg every 4 days, and DOX/Fe_3O_4/BSA-DEX-FA nanoparticle solution with DOX doses of 5, 8, and 10 mg/kg every 4 days were separately injected via the tail veins. After each administration, each mouse in DOX/Fe_3O_4/BSA-DEX-FA+field groups was immediately treated with an external magnetic field of 0.15 T closed to the tumor for 2 h. The survivability rate (SR) was calculated according to the following equation: SR (%) = (T/C − 1) × 100%, where T is the average survivable time of the DOX treated group and C is the average survivable time of the physiological saline treated group.

2.8 *In vivo* tumor MRI

The animal experiments on MRI of this study were performed at Department of Laboratory Animal Science of Fudan University in full compliance with the guidelines approved by Shanghai Administration of Experimental Animals. Male SPF BALB/c nude mice (about 20 g) were from Shanghai SLAC Lab. Animal Co. Ltd. The nude mice were injected in right axilla with 2×10^6 KB cells suspended in physiological saline. The nude mice bearing KB cells were allowed to grow for 2 weeks. Afterwards, the tumors were taken out, cut into small pieces (about 1 mm^3), and then implanted into the right hindquarter of normal nude mice. After 2 weeks of the implantation, the volume of the tumor reached to about 0.5 cm^3. Before being fixed in a stereotaxic apparatus for MRI, each mouse was anesthetized by intraperitoneal injection with 10% chloral hydrate solution at a dose of 400 mg/kg, then, 0.2 mL Fe_3O_4/BSA-DEX-FA nanoparticle solution with a iron concentration of 0.52 mg/mL was injected via the tail vein. After nanoparticle injection, the

mouse was immediately treated with an external magnetic field of 0.15 T closed to the tumor for 2 h or not. The MR images were acquired at designed time intervals on a 3T clinical MRI instrument with an animal coil. The parameters of FR-FSE sequence are as follows: TR, 3500 ms; TE, 78 ms; matrix size, 256 × 256; slice thickness, 0.8 mm; FOV, 70 × 70 mm^2; number of acquisitions, 8.

3 Results and discussion

3.1 Preparation and characterizations of DOX/Fe_3O_4/BSA-DEX-FA nanoparticles

In this study, DOX and Fe_3O_4 loaded BSA nanoparticles with FA modified DEX surface were produced for tumor diagnosis and therapy. The fabrication process of DOX/Fe_3O_4/BSA-DEX-FA nanoparticles is illustrated in Scheme 1. BSA-DEX-FA conjugate was synthesized as described previously.[23,27] Firstly, FA was conjugated to DEX via an esterification reaction between the carboxyl group of FA and the hydroxyl group of DEX with DMAP as an activator and DCC as a coupled agent. Secondly, DEX-FA and free DEX were synchronously conjugated to BSA via Maillard reaction, in which the reducing-end carbonyl group of DEX was conjugated to the amino group of BSA and no other chemical was needed. Superparamagnetic Fe_3O_4 nanocrystals were produced via a coprecipitation method. Fe_3O_4 loaded BSA-DEX-FA nanoparticles were produced by mixing Fe_3O_4 with BSA-DEX-FA in pH 4.0 aqueous solution to allow the binding between Fe_3O_4 and the carboxyl groups of BSA followed by a heating process to induce BSA gelation. Similarly, Fe_3O_4/BSA-DEX nanoparticles without FA were produced from Fe_3O_4 and BSA-DEX conjugate. DOX was loaded into Fe_3O_4/BSA-DEX-FA and Fe_3O_4/BSA-DEX nanoparticles via diffusion after changing the solution pH from acidic to 7.4.

The Fe_3O_4 nanocrystals are not stable at physiological condition; precipitation occurs after changing the medium pH from acidic to 7.4 (Fig. 1A, bottle a). The TEM image in Fig. 1B shows that the Fe_3O_4 nanocrystals are uniform but in clusters. Whereas, the photos (Fig. 1A, bottles b–e) show that Fe_3O_4/BSA-DEX, Fe_3O_4/BSA-DEX-FA, DOX/Fe_3O_4/BSA-DEX, and DOX/Fe_3O_4/BSA-DEX-FA nanoparticles are dispersible after one month of storage in pH 7.4 aqueous solutions, indicating that the Fe_3O_4 and DOX loaded nanoparticles have good stability in pH 7.4 aqueous solution. TEM image in Fig. 1C presents dispersive spherical DOX/Fe_3O_4/BSA-DEX-FA nanoparticles. The smaller and darker Fe_3O_4 nanocrystals, which have higher electron density, are inside the nanoparticles and in cluster form. The TEM image demonstrates that Fe_3O_4 nanocrystals have been successfully loaded into BSA-DEX-FA nanoparticles. There are approximately 100 free carboxyl groups in each BSA molecule.[28] The carboxyl groups of BSA can bind with Fe_3O_4 nanocrystals at pH 4.0, which is similar to the binding between the carboxyl groups of poly(methacrylic acid) and Fe_3O_4 nanocrystals at acidic condition reported by Zhang et al.[29] The heating process can induce BSA denaturation and gelation[30] that can fix the Fe_3O_4 nanocrystals in BSA gel matrix. On the other hand, the hydrophilic DEX in the conjugate can prevent the BSA from macroscopic aggregation/gelation that results in the formation of Fe_3O_4/BSA-DEX-FA nanoparticles. DOX has a pKa of 8.2,[31] its hydrochloride salt is water-soluble, but the solubility decreases with the increase of solution pH. By virtue of the electrostatic and hydrophobic interactions between DOX and BSA,[32] DOX was loaded into Fe_3O_4/BSA-DEX-FA and Fe_3O_4/BSA-DEX nanoparticles. Table 1 shows that the DOX loading efficiencies of DOX/Fe_3O_4/BSA-DEX-FA and DOX/Fe_3O_4/BSA-DEX nanoparticles are 88.7% and 94.3%, and the loading amounts are 14.2% and 14.9%, respectively. The Fe_3O_4 contents in both DOX/Fe_3O_4/BSA-DEX-FA and DOX/Fe_3O_4/BSA-DEX nanoparticles are 9.2%. These data demonstrate that DOX and Fe_3O_4 nanocrystals have been effectively loaded into BSA-DEX-FA and BSA-DEX nanoparticles.

Table 1 shows that the R_h of DOX/Fe_3O_4/BSA-DEX-FA nanoparticles is 55 nm, which is similar to the R_h values of DOX/Fe_3O_4/BSA-DEX, Fe_3O_4/BSA-DEX-FA, and Fe_3O_4/BSA-DEX nanoparticles. After one month of storage in pH 7.4 solutions, all the nanoparticles do not change their R_h values significantly, confirming that the nanoparticles are stable in pH 7.4 aqueous solutions. The long-term stability of the nanoparticles is attributed to the hydrophilic DEX chains on the surfaces of the nanoparticles.

ζ-Potential is directly related to the surface charges of macromolecule and particle. Table 2 shows that BSA and BSA-DEX-FA are positively charged at pH 4.0 and negatively charged at pH 7.4. The absolute ζ-potential values of BSA-DEX-FA conjugate are smaller than the values of BSA. This phenomenon was also observed in casein-DEX conjugate.[33] The reason is that the highly hydratable DEX chains decrease the electrophoresis mobility of the conjugate. The ζ-potential of Fe_3O_4 nanocrystals at pH 4.0 is 38.1 mV, therefore, the Fe_3O_4 nanocrystals are dispersible at pH 4.0 solution. At pH 7.4, the Fe_3O_4 nanocrystals

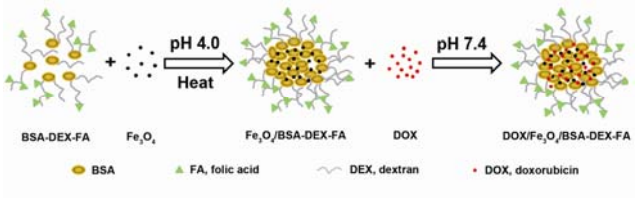

Scheme 1 Illustration of the fabrication process of Fe_3O_4/BSA-DEX-FA and DOX/Fe_3O_4/BSA-DEX-FA nanoparticles.

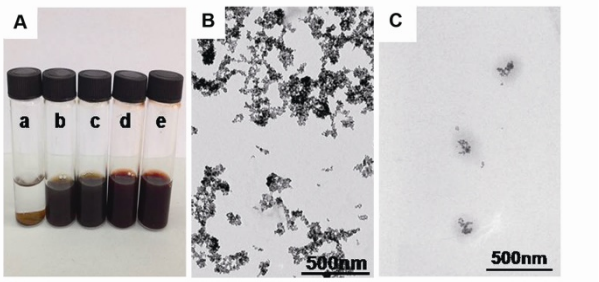

Fig. 1 (A) photos of Fe_3O_4 nanocrystals after one day of storage in pH 7.4 solution (bottle a), as well as Fe_3O_4/BSA-DEX (bottle b), Fe_3O_4/BSA-DEX-FA (bottle c), DOX/Fe_3O_4/BSA-DEX (bottle d), and DOX/Fe_3O_4/BSA-DEX-FA (bottle e) nanoparticles after one month of storage in pH 7.4 solution; TEM images of (B) Fe_3O_4 nanocrystals and (C) DOX/Fe_3O_4/BSA-DEX-FA nanoparticles. The scale bars in TEM images represent 500 nm.

Table 1 DOX loading efficiency (LE), DOX loading amount (LA), and Fe_3O_4 content in the nanoparticles; DLS results of the nanoparticles before and after one month of storage in pH 7.4 solutions.

Sample	Fresh prepared					After one month	
	R_h (nm)	PDI	LE (%)	LA (%)	Fe_3O_4 (%)	R_h (nm)	PDI
DOX/Fe_3O_4/BSA-DEX-FA	55±7	0.21±0.02	88.7±3.3	14.2±0.4	9.2±0.2	58±2	0.22±0.01
DOX/Fe_3O_4/BSA-DEX	51±1	0.17±0.01	94.3±0.2	14.9±0.2	9.2±0.2	50±1	0.19±0.01
Fe_3O_4/BSA-DEX-FA	54±1	0.17±0.01	–	–	8.2±0.2	56±1	0.21±0.02
Fe_3O_4/BSA-DEX	52±1	0.19±0.01	–	–	7.6±0.1	53±1	0.20±0.01

Table 2 ζ-Potentials of BSA, BSA-DEX-FA conjugate, Fe_3O_4 nanocrystals, Fe_3O_4/BSA-DEX-FA and DOX/Fe_3O_4/BSA-DEX-FA nanoparticles in pH 4.0 and 7.4 solutions.

Sample	ζ-Potential (mV)	
	pH 4.0	pH 7.4
BSA	8.2±1.7	–14.0±0.4
BSA-DEX-FA	5.1±0.3	–12.8±0.2
Fe_3O_4	38.1±0.6	–16.6±3.9
Fe_3O_4/BSA-DEX-FA	12.2±0.3	–15.3±0.6
DOX/Fe_3O_4/BSA-DEX-FA	–	–7.6±0.2

tend to precipitation and the ζ-potential shown in Table 2 is for reference only. The ζ-potential of Fe_3O_4/BSA-DEX-FA nanoparticles is 12.2 mV at pH 4.0, which is much smaller than the ζ-potential of Fe_3O_4 nanocrystals. This result supports the conclusion above that the Fe_3O_4 nanocrystals are embedded within BSA-DEX-FA nanoparticles. The absolute ζ-potential value of DOX/Fe_3O_4/BSA-DEX-FA nanoparticles at pH 7.4 is smaller than the value of Fe_3O_4/BSA-DEX-FA nanoparticles as a result of the binding between negative Fe_3O_4/BSA-DEX-FA and positive DOX.

The crystalline structure of the Fe_3O_4 samples was analyzed and the XRD patterns are shown in Fig. 2. The characteristic diffraction peaks of cubic Fe_3O_4 phase structure at 2θ of 30.28°, 35.75°, 43.47°, 53.93°, 57.2°, and 63.05° (JCPDS card no. 19-0629) are presented in all the patterns, confirming that the structure of Fe_3O_4 nanocrystals does not change after the loading. The size of Fe_3O_4 nanocrystals is about 10 nm calculated by Scherrer's equation[34] based on the (311) peak.

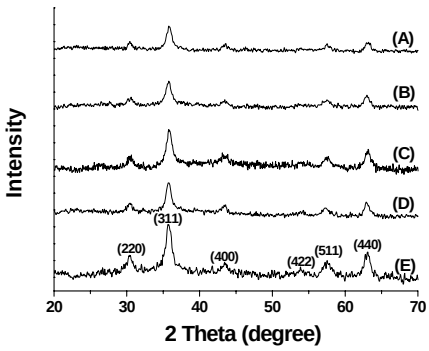

Fig. 2 XRD patterns of (A) DOX/Fe_3O_4/BSA-DEX-FA, (B) Fe_3O_4/BSA-DEX-FA, (C) DOX/Fe_3O_4/BSA-DEX, (D) Fe_3O_4/BSA-DEX, and (E) Fe_3O_4.

The magnetization curves of Fe_3O_4, DOX/Fe_3O_4/BSA-DEX-FA, and DOX/Fe_3O_4/BSA-DEX nanoparticles as a function of applied magnetic field at 300 K are shown in Fig. 3. No hysteresis loop is presented, confirming the superparamagnetic property of the nanoparticles at 300 K. Saturation magnetization (Ms) value of magnetic material determines the responsive ability under external magnetic field. The Ms values of DOX/Fe_3O_4/BSA-DEX-FA and DOX/Fe_3O_4/BSA-DEX nanoparticles are 11.6 and 10.1 emu/g, respectively, which are much smaller than 78.0 emu/g of Fe_3O_4 nanocrystals. The main reason is that the Fe_3O_4 contents in DOX/Fe_3O_4/BSA-DEX-FA and DOX/Fe_3O_4/BSA-DEX nanoparticles are lower compared with Fe_3O_4 nanocrystals. It was reported that 7–22 emu/g is usually adopted for biomedical applications,[35,36] thus, we investigated DOX/Fe_3O_4/BSA-DEX-FA as magnetically guided nanoparticles for tumor diagnosis and therapy in the following study.

3.2 *In vitro* DOX release from the nanoparticles

Fig. 4 shows the accumulative release curves of DOX from the nanoparticles. After 24 h release in pH 7.4 PBS, about 23% and 19% of the DOX were released from DOX/Fe_3O_4/BSA-DEX-FA and DOX/Fe_3O_4/BSA-DEX nanoparticles, respectively, which are much lower than the diffusion of free DOX. Table 1 shows that the loading efficiency of DOX/Fe_3O_4/BSA-DEX-FA is 88.7% and DOX/Fe_3O_4/BSA-DEX is 94.3%, which mean that DOX/Fe_3O_4/BSA-DEX-FA solution contains more free DOX. This accounts for the faster DOX releases of DOX/Fe_3O_4/BSA-DEX-FA at both pH 5.0 and 7.4 buffers. Both DOX/Fe_3O_4/BSA-DEX-FA and DOX/Fe_3O_4/BSA-DEX exhibit faster DOX release behaviours in pH 5.0 acetate buffer in comparison with the releases in pH 7.4 PBS. Because tumor cells have lower pH than normal cells,[37-39] this pH sensitive DOX release property of the nanoparticles can benefit the DOX release in tumor cells thus can decrease the side effects of DOX.

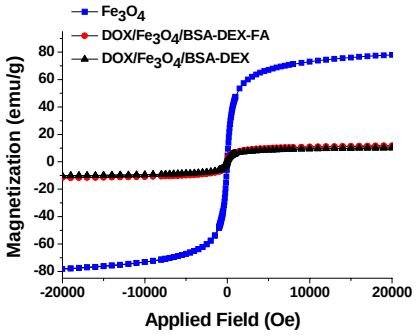

Fig. 3 Field dependent magnetization curves of Fe_3O_4, DOX/Fe_3O_4/BSA-DEX-FA, and DOX/Fe_3O_4/BSA-DEX nanoparticles at 300 K.

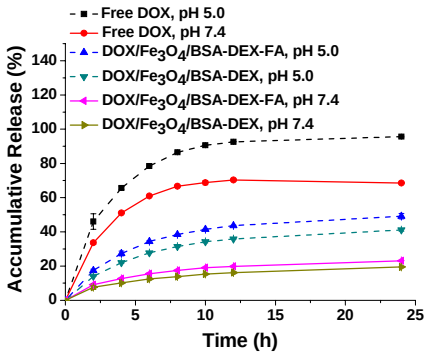

Fig. 4 Accumulative releases of DOX from the nanoparticles in 0.1 M pH 5.0 acetate buffer and pH 7.4 PBS. The free DOX was assayed as a control.

3.3 *In vitro* cytotoxicity of the nanoparticles

It was reported that FA groups can enhance the cellular uptake of the nanoparticles via folate receptor-mediated endocytosis process.[40,41] In this study, we used KB cells, which overexpress folate receptors,[42] to assay the biocompatibility of Fe_3O_4/BSA-DEX-FA and Fe_3O_4/BSA-DEX nanoparticles. Fig. 5 reveals that Fe_3O_4/BSA-DEX-FA and Fe_3O_4/BSA-DEX do not have significant cytotoxicity even at a concentration of 870 μg/mL after 48 h incubation. The good biocompatibility of Fe_3O_4/BSA-DEX-FA and Fe_3O_4/BSA-DEX nanoparticles is an important property for their biomedical applications. We also used KB cells to evaluate *in vitro* antitumor activity of DOX/Fe_3O_4/BSA-DEX-FA and DOX/Fe_3O_4/BSA-DEX nanoparticles. DOX/Fe_3O_4/BSA-DEX-FA presents better cytotoxicity than DOX/Fe_3O_4/BSA-DEX at the same DOX concentration and the same incubation time (Fig. 6), verifying the function of the FA groups in DOX/Fe_3O_4/BSA-DEX-FA nanoparticles. The cytotoxicity of DOX/Fe_3O_4/BSA-DEX-FA further increases when applying an external magnetic field of 0.17 T under the cell plate at the first 12 h of the incubation. This result indicates that external magnetic field can increase the cellular uptake of DOX/Fe_3O_4/BSA-DEX-FA, i.e., the nanoparticles have magnetically guided drug delivery function. In the DOX concentration range of 0.05–1.0 μg/mL, the antitumor activities of the DOX loaded nanoparticles are lower than the activity of free DOX (Fig. 6A). The reason is that the DOX releases from the nanoparticles are slower than the diffusion of free DOX as shown in Fig. 4. However, increasing the incubation time can increase the activity of the nanoparticles as shown in Fig. 6B. In DOX/Fe_3O_4/BSA-DEX-FA nanoparticles, the BSA molecules are crosslinked by disulfide bonds formed via disulfide–sulphydryl interchange reaction on the heating process, which is the same as BSA gelation.[32] These disulfide bonds can be cleaved in the

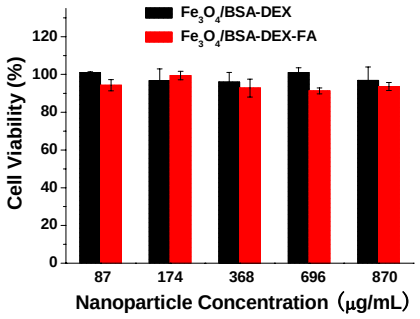

Fig. 5 Cell viabilities against different concentrations of Fe_3O_4/BSA-DEX-FA and Fe_3O_4/BSA-DEX nanoparticles after 48 h incubation.

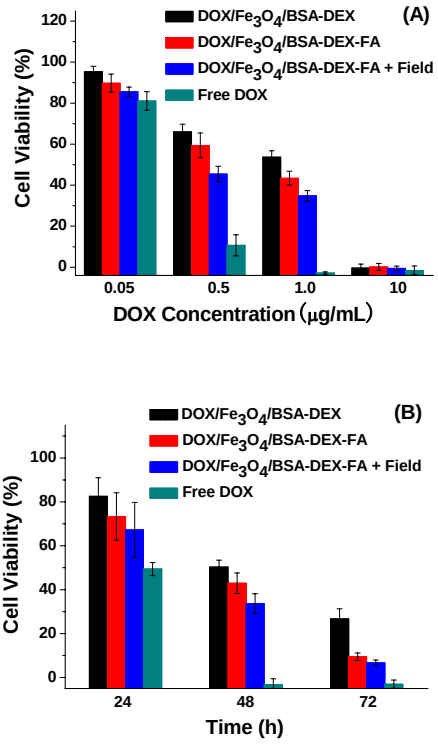

Fig. 6 (A) Cell viabilities against free DOX as well as DOX/Fe_3O_4/BSA-DEX and DOX/Fe_3O_4/BSA-DEX-FA nanoparticles at different DOX concentrations after 48 h incubation; (B) cell viabilities against free DOX as well as DOX/Fe_3O_4/BSA-DEX and DOX/Fe_3O_4/BSA-DEX-FA nanoparticles at a DOX concentration of 1.0 μg/mL after 24, 48, and 72 h incubation. The external magnetic field was applied at the first 12 h of the incubation or not.

intracellular compartments where there is 2–10 mM reducing glutathione [43] that can promote the release of the loaded DOX.

3.4 *In vitro* MRI of the nanoparticles

Nanoparticles with superparamagnetic property can be used as T_2 contrast agents which generate dark contrast in MRI.[44] The T_2-weighted images of Fe_3O_4/BSA-DEX-FA and DOX/Fe_3O_4/BSA-DEX-FA nanoparticles suspended in 1% agarose hydrogels with different Fe concentrations are shown in Fig. 7A. The MRI signal intensities of the nanoparticles decrease with the increase of the nanoparticle concentration. The R_2 relaxation rates were calculated through the linear fitting of $1/T_2$ versus Fe concentration (Fig. 7B). The R_2 values of DOX/Fe_3O_4/BSA-DEX-FA and Fe_3O_4/BSA-DEX-FA nanoparticles are 396.6 and 362.1 $(mM)^{-1}s^{-1}$, respectively. The R_2 values of current commercial MRI contrast agents are smaller than 200 $(mM)^{-1}s^{-1}$.[45-47] The much higher R_2 values obtained in this study indicate that DOX/Fe_3O_4/BSA-DEX-FA and Fe_3O_4/BSA-DEX-FA nanoparticles can afford better T_2 contrast for MRI. Fig. 8 shows the photo and T_2-weighted images of the KB cells after 6 and 24 h incubations with Fe_3O_4/BSA-DEX-FA nanoparticles in which the iron concentration was 0.052 mg/mL. With the increase of incubation time, the T_2-weighted image becomes darker because of the increase of the cellular uptake, which is confirmed by the brown colour of the cells. For the KB cells treated with an external magnetic field of 0.17 T under the cell plate, the cellular uptake of the nanoparticles increases further, and the T_2-weighted image becomes increasingly darker. These results further demonstrate that Fe_3O_4/BSA-DEX-FA nanoparticles are an efficient T_2 contrast agent and have magnetically guided function.

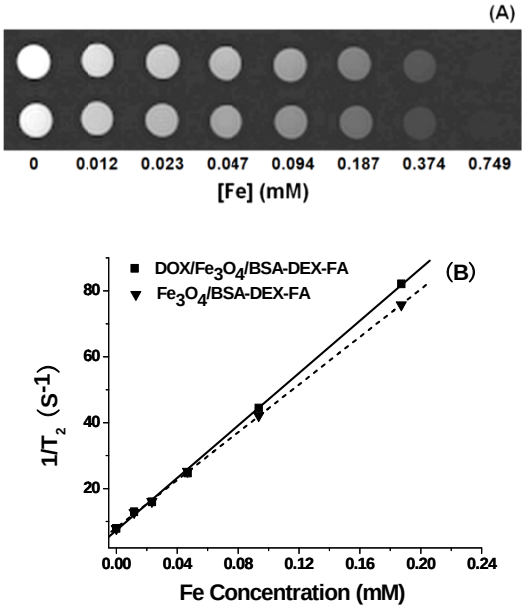

Fig. 7 (A) T_2-weighted MR images (TR = 3000 ms, TE = 13.2 ms) of Fe_3O_4/BSA-DEX-FA nanoparticles (first row) and DOX/Fe_3O_4/BSA-DEX-FA nanoparticles (second row) suspended in 1% agarose hydrogels; (B) $1/T_2$ changes of the nanoparticles as a function of Fe concentration.

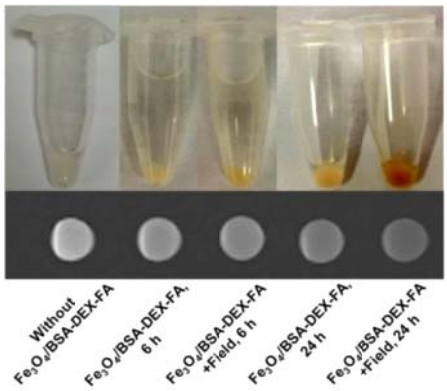

Fig. 8 Photo images of KB cells and T_2-weighted MR images (TR = 3000 ms, TE = 13.2 ms) of the cells suspended in 1% agarose hydrogels. The cells were incubated with/without Fe_3O_4/BSA-DEX-FA nanoparticles for 6 and 24 h and treated with/without an external magnetic field.

3.5 *In vivo* antitumor effect of DOX/Fe_3O_4/BSA-DEX-FA nanoparticles

It was reported that H22 cells overexpress folate receptors.[48] In this study, the tumor inhibition efficacy of DOX/Fe_3O_4/BSA-DEX-FA nanoparticles was evaluated using H22 tumor-bearing mice. H22 solid tumor grew in right axillae and the mice were treated every day for 5 days via tail veins. The tumor inhibition rates of the various treatment groups are shown in Table 3. The Fe_3O_4/BSA-DEX-FA nanoparticles, which are equivalent empty carrier for DOX dose of 8 mg/kg, have neither antitumor activity nor toxicity; the average tumor weight and average body weight of Fe_3O_4/BSA-DEX-FA group are the same as the weights of physiological saline group. For DOX/Fe_3O_4/BSA-DEX-FA group with 5 mg/kg DOX dose, the tumor inhibition rate is 48.9%, lower than the rate of 55.4% of free DOX group at the same DOX dose. However, for the free DOX group, two of the mice died during the treatment, furthermore, its average body weight of 16.9 g after the treatment is much lower than the body weight of 20.6 g of DOX/Fe_3O_4/BSA-DEX-FA group. These data indicate that DOX/Fe_3O_4/BSA-DEX-FA nanoparticles can reduce the toxicity of free DOX. Increasing DOX dose to 8 mg/kg, the tumor inhibition rate of DOX/Fe_3O_4/BSA-DEX-FA group is 49.6%, which does not increase significantly compared with the 5 mg/kg group. Applying an external magnetic field of 0.15 T closed to the tumor for 2 h after each treatment, DOX/Fe_3O_4/BSA-DEX-FA groups with DOX doses of 5 and 8 mg/kg increase their tumor inhibition rates to 54.0% and 55.9%, respectively, which are almost the same as the tumor inhibition rate of the free DOX group. This result verifies that the external magnetic field can enhance the tumor inhibition rate of DOX/Fe_3O_4/BSA-DEX-FA nanoparticles. For DOX/Fe_3O_4/BSA-DEX-FA group with 10 mg/kg DOX dose and the external magnetic field, the tumor inhibition rate is 62.8% and no mouse died during the treatment, which is superior to the free DOX group. The results in Table 3 demonstrate that DOX/Fe_3O_4/BSA-DEX-FA nanoparticles have less toxicity than free DOX, therefore, DOX/Fe_3O_4/BSA-DEX-FA can be administrated at higher dose to reach better antitumor effect.

To further evaluate the therapeutic efficacy of DOX/Fe_3O_4/BSA-DEX-FA nanoparticles, the survivability of

Table 3 H22 tumor inhibition effects of free DOX, Fe_3O_4/BSA-DEX-FA and DOX/Fe_3O_4/BSA-DEX-FA nanoparticles with/without an external magnetic field..

Group	Mice number (beginning/end)	Average body weight (g, beginning/end)	Average tumor weight (g)	Tumor inhibition rate (%)
Physiological saline	10/10	22.1/30.1	2.50±0.52	/
Fe_3O_4/BSA-DEX-FA	10/10	21.0/30.7	2.57±0.69[a]	–2.8
Free DOX (DOX 5 mg/kg)	10/8	20.9/16.9	1.11±0.54[b]	55.4
DOX/Fe_3O_4/BSA-DEX-FA (DOX 5 mg/kg)	10/10	21.5/20.6	1.28±0.50[b]	48.9
DOX/Fe_3O_4/BSA-DEX-FA (DOX 8 mg/kg)	10/10	21.2/22.2	1.26±0.54[b]	49.6
DOX/Fe_3O_4/BSA-DEX-FA + Field (DOX 5 mg/kg)	10/10	22.2/23.2	1.15±0.36[b]	54.0
DOX/Fe_3O_4/BSA-DEX-FA + Field (DOX 8 mg/kg)	10/10	19.3/19.0	1.10±0.40[b]	55.9
DOX/Fe_3O_4/BSA-DEX-FA + Field (DOX 10 mg/kg)	10/10	19.9/18.8	0.93±0.27[b]	62.8

[a] $P > 0.5$ compared with the physiological saline group.
[b] $P < 0.001$ compared with the physiological saline group.

Table 4 Survivability of H22 tumor-bearing mice after the treatments with free DOX, Fe_3O_4/BSA-DEX-FA and DOX/Fe_3O_4/BSA-DEX-FA nanoparticles with/without an external magnetic field.

Group	Average life time (d)	Survivability rate (%)
Physiological saline	12.4±1.2	/
Fe_3O_4/BSA-DEX-FA	13.0±1.1[a]	4.8
Free DOX (DOX 5 mg/kg)	15.8±3.2[b]	27.4
DOX/Fe_3O_4/BSA-DEX-FA (DOX 5 mg/kg)	14.7±4.1[a]	18.5
DOX/Fe_3O_4/BSA-DEX-FA (DOX 8 mg/kg)	17.4±3.5[b]	40.3
DOX/Fe_3O_4/BSA-DEX-FA + Field (DOX 5 mg/kg)	16.6±2.1[c]	33.9
DOX/Fe_3O_4/BSA-DEX-FA + Field (DOX 8 mg/kg)	18.4±2.0[c]	48.4
DOX/Fe_3O_4/BSA-DEX-FA + Field (DOX 10 mg/kg)	20.4±3.5[c]	64.8

[a] $P > 0.1$ compared with the physiological saline group.
[b] $P < 0.01$ compared with the physiological saline group.
[c] $P < 0.001$ compared with the physiological saline group.

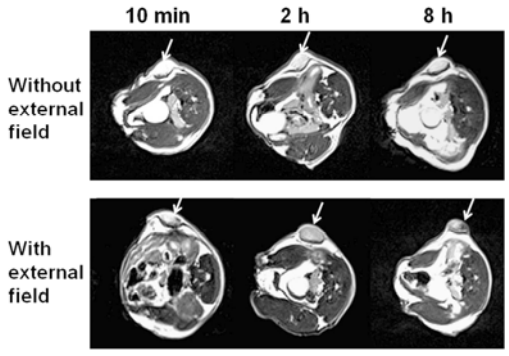

Fig. 9 T_2-weighted MR images (TR = 3500 ms, TE = 78 ms) of KB tumor-bearing mice acquired at different time intervals after injection of Fe_3O_4/BSA-DEX-FA nanoparticles. White arrow indicates tumor.

H22 tumor-bearing mice was also investigated. In survival study, H22 cells were inoculated in abdomen and grew into ascites, and the treatments were performed every 4 days via the tail veins. Table 4 shows that the average life time of DOX/Fe_3O_4/BSA-DEX-FA group is only 14.7 d, shorter than 15.8 d of free DOX group at the same DOX dose of 5 mg/kg. Increasing DOX dose to 8 mg/kg, the average life time of DOX/Fe_3O_4/BSA-DEX-FA group increases to 17.4 d. Applying an external magnetic field close to the tumor as described above, DOX/Fe_3O_4/BSA-DEX-FA groups with DOX doses of 5 and 8 mg/kg increase their average life time to 16.6 and 18.4 d, respectively. These results further verify that the external magnetic field can enhance the therapeutic efficacy of DOX/Fe_3O_4/BSA-DEX-FA nanoparticles. Increasing DOX dose to 10 mg/kg, the average life time of DOX/Fe_3O_4/BSA-DEX-FA group with the external magnetic field is 20.4 d, demonstrating that DOX/Fe_3O_4/BSA-DEX-FA nanoparticles can significantly prolong the life time of H22 tumor-bearing mice.

3.6 *In vivo* tumor MRI

In vivo MRI of tumor was performed to evaluate the contrast effect of Fe_3O_4/BSA-DEX-FA nanoparticles. Fig. 9 shows the T_2-weighted MR images of KB tumor-bearing nude mice after treatment with Fe_3O_4/BSA-DEX-FA via tail vein. The contrast effects of the images taken at 2 and 8 h post-injection are better than the contrast effect of the image taken at 10 min. This result indicates that the Fe_3O_4/BSA-DEX-FA concentration in the tumor tissue increases from 10 min to 8 h. When applying the

external magnetic field close to the tumor, the T_2 contrast between tumor tissue and normal tissue further enhances, further demonstrating that Fe_3O_4/BSA-DEX-FA concentration in the tumor tissue can be enhanced by the external magnetic field. The contrast effects shown in Fig. 9 suggest that Fe_3O_4/BSA-DEX-FA nanoparticles are a suitable contrast agent for tumor diagnosis. Furthermore, we can deduce that DOX/Fe_3O_4/BSA-DEX-FA nanoparticles can also be a MRI contrast agent. The reason is that at DOX dose of 8 mg/kg, DOX/Fe_3O_4/BSA-DEX-FA nanoparticles have the same iron concentration as in the MRI. It is possible that during the tumor treatment with DOX/Fe_3O_4/BSA-DEX-FA nanoparticles, MR images can be acquired synchronously to monitor the efficiency of treatment.

4 Conclusions

Novel multifunctional Fe_3O_4/BSA-DEX-FA and DOX/Fe_3O_4/BSA-DEX-FA nanoparticles were fabricated via a green approach for tumor MRI and therapy. Fe_3O_4/BSA-DEX-FA and DOX/Fe_3O_4/BSA-DEX-FA nanoparticles have FA modified DEX surface, a size about 100 nm, good dispersibility, excellent R_2 relaxation rate, and FA receptor-targeted and magnetically guided functions. By applying an external magnetic field close to tumor, DOX/Fe_3O_4/BSA-DEX-FA nanoparticles can effectively enhance the tumor inhibition rate and prolong the life time of H22 tumor-bearing mice; Fe_3O_4/BSA-DEX-FA nanoparticles, which have excellent biocompatibility, can effectively improve the tumor MRI of KB tumor-bearing mice. This study demonstrates that Fe_3O_4/BSA-DEX-FA and DOX/Fe_3O_4/BSA-DEX-FA nanoparticles are suitable systems for tumor diagnosis and therapy.

Acknowledgments

Financial supports of Ministry of Science and Technology of China (2011CB932503), National Natural Science Foundation of China (NSFC Project 21274026), and Key Project of the National Twelfth-Five Year Research Program of China (2012ZX09304004) are gratefully acknowledged.

Notes and references

[a] *State Key Laboratory of Molecular Engineering of Polymers and Department of Macromolecular Science, Fudan University, Shanghai 200433, China*
[b] *National Pharmaceutical Engineering Research Center, Shanghai 201203, China*
[c] *School of Materials and Chemical Engineering, West Anhui University, Liu'an, 237012, China*
* Correspondence to Ping Yao. E-mail: yaoping@fudan.edu.cn; Phone: 86-21-65642964; Fax: 86-21-65640293

1. G. L. G. Miklos, *Nat. Biotechnol.*, 2005, **23**, 535-537.
2. H. Maeda, G. Y. Bharate and J. Daruwalla, *Eur. J. Pharm. Biopharm.*, 2009, **71**, 409-419.
3. C. Sun, C. Fang, Z. Stephen, O. Veiseh, S. Hansen, D. Lee, R. G. Ellenbogen, J. Olson and M. Q. Zhang, *Nanomedicine*, 2008, **3**, 495-505.
4. M. Ferrari, *Nat. Rev. Cancer*, 2005, **5**, 161-171.
5. A. Shalviri, W. D. Foltz, P. Cai, A. M. Rauth and X. Y. Wu, *J. Controlled Release*, 2013, **167**, 11-20.
6. C. Wang, H. Xu, C. Liang, Y. M. Liu, Z. W. Li, G. B. Yang, H. Cheng, Y. G. Li and Z. Liu, *ACS nano*, 2013, **7**, 6782-6795.
7. B. H. Kim, N. Lee, H. Kim, K. An, Y. I. Park, Y. Choi, K. Shin, Y. Lee, S. G. Kwon, H. B. Na, J. G. Park, T. Y. Ahn, Y. W. Kim, W. K. Moon, S. H. Choi and T. Hyeon, *J. Am. Chem. Soc.*, 2011, **133**, 12624-12631.
8. Y. Yu and D. Sun, *Expert Review of Clinical Pharmacology*, 2010, **3**, 117-130.
9. D. H. Kim, E. A. Rozhkova, I. V. Ulasov, S. D. Bader, T. Rajh, M. S. Lesniak and V. Novosad, *Nat. Mater.*, 2010, **9**, 165-171.
10. J. Gautier, E. Allard-Vannier, E. Munnier, M. Souce and I. Chourpa, *J. Controlled Release*, 2013, **169**, 48-61.
11. L. L. Zhou, J. Y. Yuan and Y. Wei, *J. Mater. Chem.*, 2011, **21**, 2823-2840.
12. C. Huang, K. G. Neoh, E. T. Kang and B. Shuter, *J. Mater. Chem.*, 2011, **21**, 16094-16102.
13. C. Huang, Z. M. Tang, Y. B. Zhou, X. F. Zhou, Y. Jin, D. Li, Y. Yang and S. B. Zhou, *Int. J. Pharm.*, 2012, **429**, 113-122.
14. A. Gianella, P. A. Jarzyna, V. Mani, S. Ramachandran, C. Calcagno, J. Tang, B. Kann, W. J. R. Dijk, V. L. Thijssen, A. W. Griffioen, G. Storm, Z. A. Fayad and W. J. M. Mulder, *ACS nano*, 2011, **5**, 4422-4433.
15. V. T. G. Chuang, U. Kragh-Hansen and M. Otagiri, *Pharm. Res.*, 2002, **19**, 569-577.
16. F. Kratz, *J. Controlled Release*, 2008, **132**, 171-183.
17. F. Wu, S. A. Wuensch, M. Azadniv, M. R. Ebrahimkhani and I. N. Crispe, *Molecular pharmaceutics*, 2009, **6**, 1506-1517.
18. B. Elsadek and F. Kratz, *J. Controlled Release*, 2012, **157**, 4-28.
19. S. Wagner, F. Rothweiler, M. G. Anhorn, D. Sauer, I. Riemann, E. C. Weiss, A. Katsen-Globa, M. Michaelis, J. Cinatl, D. Schwartz, J. Kreuter, H. von Briesen and K. Langer, *Biomaterials*, 2010, **31**, 2388-2398.
20. S. Bae, K. Ma, T. H. Kim, E. S. Lee, K. T. Oh, E. S. Park, K. C. Lee and Y. S. Youn, *Biomaterials*, 2012, **33**, 1536-1546.
21. J. Wang, Z. H. Zhang, X. Wang, W. Wu and X. Q. Jiang, *J. Controlled Release*, 2013, **168**, 1-9.
22. B. B. Zhang, Q. Li, P. H. Yin, Y. P. Rui, Y. Y. Qiu, Y. Wang and D. L. Shi, *ACS Appl. Mat. Interfaces*, 2012, **4**, 6479-6486.
23. H. Q. Hao, Q. M. Ma, C. Huang, F. He and P. Yao, *Int. J. Pharm.*, 2013, **444**, 77-84.
24. K. M. Laginha, S. Verwoert, G. J. R. Charrois and T. M. Allen, *Clin. Cancer Res.*, 2005, **11**, 6944-6949.
25. S. M. Sagnella, H. Duong, A. MacMillan, C. Boyer, R. Whan, J. A. McCarroll, T. P. Davis and M. Kavallaris, *Biomacromolecules*, 2014, **15**, 262-275.
26. F. Sauzedde, A. Elaissari and C. Pichot, *Colloid. Polym. Sci.*, 1999, **277**, 846-855.
27. H. Q. Hao and P. Yao, *Chem. J. Chin. Univ.-Chin.*, 2014, **35**, 652-659.
28. H. A. Saroff, N. R. Rosenthal, E. R. Adamik, N. Hages and H. A. Scheraga, *J. Biol. Chem.*, 1953, **205**, 255-270.
29. H. Zhang, R. B. Wang, G. Zhang and B. Yang, *Thin Solid Films*, 2003, **429**, 167-173.
30. J. I. Boye, I. Alli and A. A. Ismail, *J. Agric. Food. Chem.*, 1996, **44**, 996-1004.
31. S. C. Yang, H. X. Ge, Y. Hu, X. Q. Jiang and C. Z. Yang, *J. Appl. Polym. Sci.*, 2000, **78**, 517-526.
32. J. N. Qi, P. Yao, F. He, C. L. Yu and C. O. Huang, *Int. J. Pharm.*, 2010, **393**, 176-184.
33. X. Y. Pan, M. F. Mu, B. Hu, P. Yao and M. Jiang, *Biopolymers*, 2006, **81**, 29-38.
34. M. Das, D. Mishra, T. K. Maiti, A. Basak and P. Pramanik, *Nanotechnology*, 2008, **19**, 415101.
35. Q. L. Fan, K. G. Neoh, E. T. Kang, B. Shuter and S. C. Wang, *Biomaterials*, 2007, **28**, 5426-5436.
36. P. Tartaj and C. J. Serna, *J. Am. Chem. Soc.*, 2003, **125**, 15754-15755.
37. L. E. Gerweck and K. Seetharaman, *Cancer Res.*, 1996, **56**, 1194-1198.
38. J. Pouyssegur, F. Dayan and N. M. Mazure, *Nature*, 2006, **441**, 437-443.

39. S. Ganta, H. Devalapally, A. Shahiwala and M. Amiji, *J. Controlled Release*, 2008, **126**, 187-204.
40. H. S. Yoo and T. G. Park, *J. Controlled Release*, 2004, **96**, 273-283.
41. S. H. Kim, J. H. Jeong, C. O. Joe and T. G. Park, *J. Controlled Release*, 2005, **103**, 625-634.
42. S. Nayak, H. Lee, J. Chmielewski and L. A. Lyon, *J. Am. Chem. Soc.*, 2004, **126**, 10258-10259.
43. H. L. Sun, B. N. Guo, X. Q. Li, R. Cheng, F. H. Meng, H. Y. Liu and Z. Y. Zhong, *Biomacromolecules*, 2010, **11**, 848-854.
44. H. B. Na, I. C. Song and T. Hyeon, *Adv. Mater.*, 2009, **21**, 2133-2148.
45. M. Rohrer, H. Bauer, J. Mintorovitch, M. Requardt and H. J. Weinmann, *Invest. Radiol.*, 2005, **40**, 715-724.
46. Y. X. J. Wang, S. M. Hussain and G. P. Krestin, *Eur. Radiol.*, 2001, **11**, 2319-2331.
47. T. Allkemper, C. Bremer, L. Matuszewski, W. Ebert and P. Reimer, *Radiology*, 2002, **223**, 432-438.
48. L. He and Q. L. Zhu, *Chinese Pharmaceutical Journal*, 2010, **45**, 107-110.

Graphical Abstract

Doxorubicin loaded albumin nanoparticles with folic acid receptor-targeted and magnetically guided functions significantly improve tumor therapy and MRI.